ELSEVIER

Journal of Fluids and Structures 25 (2009) 519–534

JOURNAL OF FLUIDS AND STRUCTURES

www.elsevier.com/locate/jfs

Multi-parameter aerodynamic modeling for aeroelastic coupling in turbomachinery

D.-M. Tran*

Aeroelasticity and Structural Dynamics Department, ONERA, The French Aerospace Lab, B.P. 72, 29 avenue de la Division Leclerc, 92322 Châtillon Cedex, France

Received 12 March 2007; accepted 19 September 2008
Available online 5 March 2009

Abstract

A multi-parameter method based on multivariate spline function approximation and minimum state smoothing for modeling the generalized aerodynamic forces is proposed in order to reduce the cost of the aerodynamic computations in the solution of the coupled fluid–structure problem in turbomachinery. This method allows simultaneous variations of several parameters and provides the solutions of the coupled systems at arbitrary values of the parameters using the generalized aerodynamic forces computed at the few values of the parameters. This multi-parameter aerodynamic modeling method is applied to a large-chord blade, for which the two chosen parameters are the rotation speed and the inter-blade phase angle.

Keywords: Fluid–structure coupling; Linearized aerodynamics; Aeroelasticity; Turbomachinery; Multivariate spline

1. Introduction

This paper is concerned with the coupled fluid–structure dynamic analysis problem in turbomachinery, i.e. the interaction between the structural motion and the surrounding unsteady flow, whose a review of the solution methods can be found in Marshall and Imregun (1996).

In a previous work (Tran et al., 2003), two indirect coupling methods were proposed, they are based on the cyclic symmetry properties of both structure and fluid (Thomas, 1979; Valid and Ohayon, 1985), so that the reduction of the analysis to only one structural reference sector and one fluid channel can be applied. The equation of motion of a reference sector in the traveling wave coordinates is projected on the complex modes of the undamped structure in vacuum to obtain a reduced coupled system for each phase number. The unsteady aerodynamic forces are assumed to depend linearly on the structural displacements and velocities, and they are computed prior to the coupling calculations by solving the Euler equations and by imposing a harmonic motion to the modes, for an inter-blade phase angle and for several reduced oscillation frequencies. The reduced coupled system is then solved by using either the double scanning method (or $p-k$ method) in the frequency domain (Dat and Meurzec, 1969), or Karpel's minimum state smoothing method (Karpel, 1982; Roberts, 1991; Poirion, 1995) in both frequency and time domains. Structural nonlinearities such as friction or free-play can be taken into account (Liauzun and Tran, 2002; Tran and Liauzun, 2003) by using Craig and Bampton's projection basis (Craig and Bampton, 1968; Tran, 2001).

*Tel.: +33 1 46 73 46 32; fax: +33 1 46 73 41 43.
E-mail address: tran@onera.fr

0889-9746/$ - see front matter
doi:10.1016/j.jfluidstructs.2008.09.001

The proposed indirect coupling methods are more sophisticated than the uncoupled approach which assumes that there is no aerodynamic coupling between the modes and that the aerodynamic forces remain unchanged whether the structure is under aerodynamic loads or not, and by consequent, the aerodynamic forces are only computed for each mode in vacuum which oscillates at its eigenfrequency and they are then introduced as constant scalars in the decoupled modal equations in order to deduce the aeroelastic damping and stability of the modes (Crawley, 1988). The proposed indirect coupling methods take into account the aeroelastic coupling between the modes and the dependence of the aerodynamic forces on the structural motion under aerodynamic loads and especially on the unknown aeroelastic eigenvalues, leading to a nonlinear eigenvalue problem which requires iterative solutions in the case of the flutter equation. However, the aerodynamic forces are determined only once at the beginning of the simulation for the modes in vacuum and the structural motion does not interact directly on the aerodynamic forces but only via the structural modes, thanks to the hypotheses of linearized aerodynamics and harmonic motion. These assumptions are removed in the direct coupling method where the structural motion equation, projected or not on the modes, and the fluid equations are solved alternatively at each time step, with the data transferred from one computation to the next one (as boundary conditions or pressure load) via the fluid–structure interface (Jacquet-Richardet and Rieutord, 1998; Grisval and Liauzun, 1999, 2000; Sayma et al., 2000; Carstens et al., 2003; Gnesin et al., 2004; Dugeai, 2005, 2008). The results of the indirect and direct coupling methods were compared in Tran et al. (2003) for an inviscid flow, and in Moffatt and He (2005) for a viscous flow. Other works related to the aeroelastic coupling in turbomachinery propose to construct reduced order models of the fluid (Willcox, 2000; Epureanu et al., 2000, 2001; Epureanu, 2003; Sarkar and Venkatraman, 2004; Attar and Dowell, 2005) which constitute an alternative solution to the present work for reducing the aerodynamic computational cost, or to take into account the mistuning of the blades (He et al., 2007, 2008).

In order to detect the instability areas in the turbomachinery operation map, the aerodynamic and coupling calculations should be performed at several points by varying several parameters such as the inlet/outlet pressure ratio, the rotation speed, the inter-blade phase angle, the excited mode, the excitation frequency, etc. As an example, a direct coupling method which includes the inter-blade phase angle at which stability or instability would occur as a part of solution was proposed in Rzadkowski and Gnesin (2007). For each point in the operation map and for each value of the parameters, aerodynamic computations should be performed to generate the generalized aerodynamic forces (GAF) that are needed in the coupled system. This leads to an important number of aerodynamic computations which are the most time consuming tasks for obtaining the solutions of the coupled fluid–structure problem. In order to reduce the number and therefore the cost of the aerodynamic computations, a multi-parameter method for modeling the GAF is proposed. This method, which has already been applied to aircraft applications (Poirion, 1996), uses at first a spline function approximation (de Boor, 1992, 2001) of the GAF in terms of the chosen parameter, and then Karpel's minimum state smoothing of the spline coefficient matrices. The first version using univariate spline approximation of this method has been developed and applied to turbomachinery blades with only one parameter which is the rotation speed (Tran et al., 2004, 2005).

The aim of this paper is to propose a multi-parameter method using multivariate spline approximation and Karpel's minimum state smoothing for modeling the GAF in order to reduce more and more the cost of aerodynamic computations. This method allows simultaneous variations of several parameters and provides the solutions of the coupled systems at arbitrary "computed" values of the parameters from the GAF computed at the few "initial" values of the parameters, without any additional aerodynamic computations. It also allows both interpolation and extrapolation, this means that the computed values of the parameters can lay inside or outside the domain defined by the initial values. This extrapolation capability is very useful since it makes easier the detection of unstable areas in the operation map, which are generally localized at the outskirts of the stable area, and where the aerodynamic computations generally fail to converge.

This paper is organized as follows: the reduced coupled system and the multivariate spline approximation of the GAF are presented in Section 2. The multi-parameter Karpel's minimum state modeling of the reduced coupled system using multivariate spline approximation is presented in Section 3. In Section 4, the multi-parameter aerodynamic modeling method is applied to an aircraft engine compressor blade, for which the two chosen parameters are the rotation speed and the inter-blade phase angle. The results obtained with this method at the computed values of the parameters will be compared to the reference results obtained by performing the aerodynamic computations at these values.

2. Reduced coupled system and multivariate spline approximation of GAF

2.1. Reduced coupled system

A structure with cyclic symmetry is composed of N identical sectors $S_0, S_1, \ldots, S_{N-1}$ which close up on themselves to form a circular system. The whole structure is obtained by $N-1$ repeated rotations of a reference sector S_0 through the

angle $\beta = 2\pi/N$. Each sector is limited by a left and a right frontier L_l and L_r with the adjacent sectors. The fluid surrounding the structure is also assumed to have the same cyclic symmetry while the applied external forces can vary arbitrarily from one sector to another sector.

Using the cyclic symmetry properties, the equation of motion of the structure comes down to N motion equations of the reference sector S_0, in terms of the traveling wave coordinates $\mathbf{u}_n$ and with the appropriate second members and boundary conditions for N phase numbers $n = 0, \ldots, N-1$ and the associated inter-blade phase angles $\sigma_n = n\beta$. For each phase number n, by expressing $\mathbf{u}_n$ as a linear combination of the first m_n complex modes $\mathbf{\Phi}_n$ of the undamped, rotating structure in vacuum, $\mathbf{u}_n = \mathbf{\Phi}_n \mathbf{q}_n$, and by projecting the motion equation of S_0 on $\mathbf{\Phi}_n$, we obtain the reduced coupled system in the m_n complex modal coordinates $\mathbf{q}_n(t)$ in the time domain:

$$\mathbf{K}_{gn}\mathbf{q}_n + \mathbf{C}_{gn}\dot{\mathbf{q}}_n + \mathbf{M}_{gn}\ddot{\mathbf{q}}_n = \mathbf{f}_{agn}(\mathbf{\Phi}_n\mathbf{q}_n, \mathbf{\Phi}_n\dot{\mathbf{q}}_n) + \mathbf{f}_{gn}, \tag{1}$$

where $\mathbf{K}_{gn}$ and $\mathbf{M}_{gn}$ are the diagonal, real generalized stiffness and mass matrices, $\mathbf{C}_{gn}$ is the complex generalized damping and gyroscopic effect matrix, $\mathbf{f}_{agn}$ and $\mathbf{f}_{gn}$ are the complex generalized aerodynamic and external forces.

For the aeroelastic stability analysis, all the external forces are null except the aerodynamic forces. The solutions are looked up under the form $\mathbf{q}_n(t) = \tilde{\mathbf{q}}_n e^{pt}$ with $p = i\omega(1 + i\alpha)$ where $\omega > 0$ and $\alpha \in \mathbb{R}$ are the unknown aeroelastic eigenfrequency and damping factor. Using the hypothesis of linearity, the GAF are written as $\mathbf{f}_{agn}(\mathbf{\Phi}_n \mathbf{q}_n, \mathbf{\Phi}_n \dot{\mathbf{q}}_n) = \tilde{\mathbf{F}}_{agn}(\mathbf{\Phi}_n, p)\,\tilde{\mathbf{q}}_n e^{pt}$ and Eq. (1) leads to the flutter equation:

$$[\mathbf{K}_{gn} + p\mathbf{C}_{gn} + p^2\mathbf{M}_{gn} - \tilde{\mathbf{F}}_{agn}(\mathbf{\Phi}_n, p)]\tilde{\mathbf{q}}_n = \mathbf{0}, \tag{2}$$

which is a complex, nonlinear eigenvalue system in which the aerodynamic coefficient matrix $\tilde{\mathbf{F}}_{agn}(\mathbf{\Phi}_n, p)$ depends on the complex modes $\mathbf{\Phi}_n$ and the unknown complex eigenvalue p.

The unsteady aerodynamic forces are computed from a basis of real mode shapes $\mathbf{\Psi}$ of the reference sector, for an oscillation frequency ω and an inter-blade phase angle σ_n. By imposing a harmonic motion to the modes $\mathbf{\Psi}$ and by assuming that all the sectors have the same motion with a constant phase angle σ_n between two adjacent sectors, we obtain the time-dependent aerodynamic coefficient matrix $\mathbf{F}_{agn}(\mathbf{\Psi}, i\omega, t) = -\frac{1}{2}\rho_\infty V_\infty^2 \mathbf{A}_n(\mathbf{\Psi}, i\omega, t)$ whose (i,j)-term is obtained by projecting the unsteady aerodynamic force generated by the harmonic motion of the jth mode on the ith mode, and where ρ_∞ and V_∞ are the density and the velocity of the upstream unperturbed fluid. By keeping the first harmonic term in the Fourier analysis of $\mathbf{F}_{agn}(\mathbf{\Psi}, i\omega, t)$, we have

$$\mathbf{F}_{agn}(\mathbf{\Psi}, i\omega, t) \simeq \tilde{\mathbf{F}}_{agn}(\mathbf{\Psi}, i\omega)e^{i\omega t} = -\tfrac{1}{2}\rho_\infty V_\infty^2 \tilde{\mathbf{A}}_n(\mathbf{\Psi}, i\omega)e^{i\omega t}.$$

$\tilde{\mathbf{F}}_{agn}(\mathbf{\Psi}, i\omega)$ and $\tilde{\mathbf{A}}_n(\mathbf{\Psi}, i\omega)$ are complex, asymmetric square matrices of dimension m_n. They are computed for n_ω oscillation frequencies $\omega_1, \ldots, \omega_{n_\omega}$. The aerodynamic coefficient matrix $\tilde{\mathbf{F}}_{agn}(\mathbf{\Phi}_n, i\omega)$ generated by the complex modes $\mathbf{\Phi}_n$ in Eq. (2) can be recomposed from the aerodynamic coefficient matrix obtained with the real and imaginary parts of $\mathbf{\Phi}_n$ by using the linearity hypothesis (Tran et al., 2003).

2.2. Multivariate spline approximation of GAF

We consider the aerodynamic coefficient matrix $\tilde{\mathbf{A}}_n(\mathbf{\Phi}_n, p, x, y)$ associated with a modal basis $\mathbf{\Phi}_n$, which depends on the unknown complex eigenvalue p and also on two parameters x and y. For the sake of simplicity, the multivariate spline approximation of the GAF is presented here for the case of two variables, however, the generalization to the case of more than two variables is immediate. The symbol $\mathbf{\Phi}_n$ is also removed from the expression of $\tilde{\mathbf{A}}_n$.

Let us define the reduced frequency $\kappa = \omega c/V_\infty$, where c is a reference length, for example the blade chord. Let $K = \{\kappa_1 < \cdots < \kappa_{n_\kappa}\}$, $T_x = \{x_1 < \cdots < x_{n_x}\}$ and $T_y = \{y_1 < \cdots < y_{n_y}\}$ be the reduced frequencies and the initial values of the parameters for which the aerodynamic coefficient matrices have been computed (tabulated). The number and the values of the reduced frequencies should be the same for all the parameters. Any couple of initial values $(x_i, y_j) \in T_x \times T_y$ of the parameters is called an initial point. The aerodynamic coefficient matrix computed with the excitation frequency ω or the reduced frequency κ and for the initial points (x_i, y_j) is denoted by $\tilde{\mathbf{A}}_n(i\omega, x_i, y_j)$ or $\tilde{\mathbf{A}}_n(i\kappa, x_i, y_j)$.

We look for an approximation (interpolation and extrapolation) formulation in x and y, which is defined simultaneously for all the reduced frequencies $\kappa_1, \ldots, \kappa_{n_\kappa}$.

Let us define the complex vector of dimension $(m_n^2 n_\kappa \times 1)$, which is formed by the columns of the matrices $\tilde{\mathbf{A}}_n(i\kappa_1, x_i, y_j), \ldots, \tilde{\mathbf{A}}_n(i\kappa_{n_\kappa}, x_i, y_j)$:

$$\mathbf{a}_n(x_i, y_j) = {}^t[{}^t\tilde{\mathbf{A}}_n(i\kappa_1, x_i, y_j)_{\bullet,1}, \ldots, {}^t\tilde{\mathbf{A}}_n(i\kappa_1, x_i, y_j)_{\bullet,m_n}, \ldots, {}^t\tilde{\mathbf{A}}_n(i\kappa_{n_\kappa}, x_i, y_j)_{\bullet,1}, \ldots, {}^t\tilde{\mathbf{A}}_n(i\kappa_{n_\kappa}, x_i, y_j)_{\bullet,m_n}], \tag{3}$$

where $\tilde{\mathbf{A}}_n(i\kappa_j, x_i, y_j)_{\bullet,l}$ denotes the lth column of $\tilde{\mathbf{A}}_n(i\kappa_j, x_i, y_j)$.

The vector function $\mathbb{R}\times\mathbb{R}\longrightarrow\mathbb{C}^{m_n^2 n_\kappa}$, $(x,y)\mapsto\mathbf{a}_n(x,y)$, which has been obtained at the initial points $(x_i,y_j)\in T_x\times T_y$, can be extended to the domain $[x_{\min},x_{\max}]\times[y_{\min},y_{\max}]$ by using a two-variate spline function approximation (de Boor, 1992, 2001):

$$\mathbf{a}_n(x,y)=\sum_{s=1}^{n_y}\sum_{r=1}^{n_x}B_{rs}(x,y)\mathbf{b}_{r,s}\quad\text{for }(x,y)\in[x_{\min},x_{\max}]\times[y_{\min},y_{\max}],\tag{4}$$

where (x,y) is any arbitrary couple of computed values of the parameters and it is called a computed point, while $x_{\min}$, $x_{\max}$, $y_{\min}$ and $y_{\max}$ are the minimum and maximum computed values of the parameters for which the coupling computations will be performed. These values do not need to belong to the domain defined by the initial values, in particular when an extrapolation of the function is required. The two-variate real functions B_{rs} are products of univariate B-spline functions which are associated with the sequences of knots $T'_x=\{x'_1\leqslant\cdots\leqslant x'_{n_x+k_x}\}$ and $T'_y=\{y'_1\leqslant\cdots\leqslant y'_{n_y+k_y}\}$, the latters depend only on the orders k_x and k_y of the B-spline functions and on the initial values T_x and T_y. The knots x'_1, $x'_{n_x+k_x}$, y'_1 and $y'_{n_y+k_y}$ at the extremities of T'_x and T'_y, with multiplicity k_x and k_y, are chosen so that $x'_1\leqslant\min(x_{\min},x_1)$, $x'_{n_x+k_x}\geqslant\max(x_{\max},x_{n_x})$,$y'_1\leqslant\min(y_{\min},y_1)$ and $y'_{n_y+k_y}\geqslant\max(y_{\max},y_{n_y})$. The complex spline coefficient vectors $\mathbf{b}_{r,s}$ depend on k_x, k_y, T'_x, T'_y and the tabulated data $\mathbf{a}_n(x_i,y_j)$ at the initial points.

For each computed point (x,y), the vector $\mathbf{a}_n(x,y)$ can be then reshaped using the inverse transformation of Eq. (3) to obtain n_κ complex aerodynamic coefficient matrices $\tilde{\mathbf{A}}_n(\mathrm{i}\kappa_1,x,y),\ldots,\tilde{\mathbf{A}}_n(\mathrm{i}\kappa_{n_\kappa},x,y)$ of dimension $(m_n\times m_n)$:

$$\tilde{\mathbf{A}}_n(\mathrm{i}\kappa_1,x,y)=[\mathbf{a}_{n,1}(x,y),\ldots,\mathbf{a}_{n,m_n}(x,y)],\ldots,\tilde{\mathbf{A}}_n(\mathrm{i}\kappa_{n_\kappa},x,y)=[\mathbf{a}_{n,(n_\kappa-1)\,m_n+1}(x,y),\ldots,\mathbf{a}_{n,n_\kappa\,m_n}(x,y)],\tag{5}$$

where $\mathbf{a}_{n,j}$ is the jth bloc of dimension $(m_n\times 1)$ of the vector $\mathbf{a}_n(x,y)$.

3. Multi-parameter minimum state modeling of the reduced coupled system

In the previous section, the aerodynamic coefficient matrices $\tilde{\mathbf{A}}_n(\mathrm{i}\omega,x,y)$ have been obtained from the spline approximation equations (4) and (5), for n_κ reduced frequencies and with the assumption of harmonic motion. The reduced coupled system can be then solved at any arbitrary computed point (x,y) in both frequency and time domains by using either the double scanning method or Karpel's minimum state smoothing method (Tran et al., 2003). For arbitrary motions like those defined in Eqs. (1) and (2) the minimum state smoothing method (Karpel, 1982) provides an extension of the aerodynamic coefficient matrix to an area of the complex plane containing the imaginary axis, i.e. to determine $\tilde{\mathbf{A}}_n(p,x,y)$ for $p=\mathrm{i}\omega(1+\mathrm{i}\alpha)$ with $\alpha\neq 0$. It consists in modeling the GAF by using a rational approximation and auxiliary state variables:

$$\tilde{\mathbf{A}}_n(p,x,y)\simeq\mathbf{A}_{n0}+\frac{pc}{V_\infty}\mathbf{A}_{n1}+\frac{p^2c^2}{V_\infty^2}\mathbf{A}_{n2}+\frac{pc}{V_\infty}\mathbf{D}_n\left[\frac{pc}{V_\infty}\mathbf{I}-\mathbf{R}_n\right]^{-1}\mathbf{E}_n.\tag{6}$$

The matrices $\mathbf{A}_{n0}$, $\mathbf{A}_{n1}$, $\mathbf{A}_{n2}$, $\mathbf{D}_n$, $\mathbf{R}_n$ and $\mathbf{E}_n$ are real with dimensions $(m_n\times m_n)$ for $\mathbf{A}_{n0}$, $\mathbf{A}_{n1}$ and $\mathbf{A}_{n2}$, $(m_n\times n_p)$ for $\mathbf{D}_n$, $(n_p\times m_n)$ for $\mathbf{E}_n$ and $\mathbf{R}_n=\mathrm{diag}(r_1,\ldots,r_{n_p})$ where n_p is the degree of the denominator of the rational function or the number of poles and $r_i<0$ are the poles. These matrices are computed by using a method of least squares minimization (Poirion, 1995; Tran et al., 2003).

However, in this mono-parameter method, the rational approximation equation (6) should be performed for each computed point (x,y), whose number can be much more important than the number of the initial points. In this section, we propose a multi-parameter modeling of the GAF by using the spline approximation and the minimum state smoothing, in which the latter is only performed $n_x\times n_y$ times whatever the number of the computed points. We obtain a reduced coupled system which depends explicitly on the parameters and which can be solved for any arbitrary computed points in both frequency and time domains.

To this aim, we remark that the spline coefficient vectors $\mathbf{b}_{r,s}$ in Eq. (5) are similar to the vectors $\mathbf{a}_n(x_i,y_j)$ obtained in Eq. (3) from the tabulated aerodynamic coefficient matrices. In particular, these two vectors coincide if the spline functions of order 2 are used and if there is no extrapolation. We can then perform the minimum state smoothing on the spline coefficient vectors $\mathbf{b}_{r,s}$. Each vector $\mathbf{b}_{r,s}$ is first reshaped in a similar way as in Eq. (5) to obtain n_κ complex aerodynamic coefficient matrices $\mathbf{A}_{n,r,s}(\kappa_1),\ldots,\mathbf{A}_{n,r,s}(\kappa_{n_\kappa})$ of dimension $(m_n\times m_n)$:

$$\mathbf{A}_{n,r,s}(\kappa_1)=[\mathbf{b}_{r,s,1},\ldots,\mathbf{b}_{r,s,m_n}],\ldots,\mathbf{A}_{n,r,s}(\kappa_{n_\kappa})=[\mathbf{b}_{r,s,(n_\kappa-1)m_n+1},\ldots,\mathbf{b}_{r,s,n_\kappa m_n}].\tag{7}$$

3.1. Multi-parameter minimum state modeling in frequency domain

From the matrices $\mathbf{A}_{n,r,s}(\kappa_1),\ldots,\mathbf{A}_{n,r,s}(\kappa_{n_\kappa})$, Karpel's minimum state smoothing provides rational approximations of the matrices $\mathbf{A}_{n,r,s}(p)$ in the frequency domain, for $r=1,\ldots,n_x$ and $s=1,\ldots,n_y$:

$$\mathbf{A}_{n,r,s}(p) \simeq \mathbf{A}_{n0,r,s} + \frac{pc}{V_\infty}\mathbf{A}_{n1,r,s} + \frac{p^2c^2}{V_\infty^2}\mathbf{A}_{n2,r,s} + \frac{pc}{V_\infty}\mathbf{D}_{n,r,s}\left[\frac{pc}{V_\infty}\mathbf{I}-\mathbf{R}_{n,r,s}\right]^{-1}\mathbf{E}_{n,r,s}, \tag{8}$$

where the real matrices $\mathbf{A}_{n0,r,s}$, $\mathbf{A}_{n1,r,s}$, $\mathbf{A}_{n2,r,s}$, $\mathbf{D}_{n,r,s}$, $\mathbf{E}_{n,r,s}$, and $\mathbf{R}_{n,r,s}$ are similar to those in Eq. (6). Note that the number of poles $n_{p,r,s}$ can be different for each couple (r,s).

Eq. (4) is then extended to the matrices $\mathbf{A}_{n,r,s}(p)$ to obtain a spline approximation of the aerodynamic coefficient matrix in the frequency domain for any complex eigenvalue p and any arbitrary computed point (x,y):

$$\tilde{\mathbf{A}}_n(p,x,y) \simeq \sum_{r=1}^{n_x}\sum_{s=1}^{n_y} B_{r,s}(x,y)\mathbf{A}_{n,r,s}(p) \quad \text{for } (x,y)\in[x_{\min},x_{\max}]\times[y_{\min},y_{\max}]. \tag{9}$$

Substituting Eq. (8) in Eq. (9), we obtain

$$\tilde{\mathbf{A}}_n(p,x,y) \simeq \mathbf{A}_{n0}(x,y) + \frac{pc}{V_\infty}\mathbf{A}_{n1}(x,y) + \frac{p^2c^2}{V_\infty^2}\mathbf{A}_{n2}(x,y) + \sum_{r=1}^{n_x}\sum_{s=1}^{n_y} B_{r,s}(x,y)\left(\frac{pc}{V_\infty}\mathbf{D}_{n,r,s}\left[\frac{pc}{V_\infty}\mathbf{I}-\mathbf{R}_{n,r,s}\right]^{-1}\mathbf{E}_{n,r,s}\right) \tag{10}$$

with

$$\mathbf{A}_{n0}(x,y) = \sum_{r=1}^{n_x}\sum_{s=1}^{n_y} B_{r,s}(x,y)\mathbf{A}_{n0,r,s}, \quad \mathbf{A}_{n1}(x,y) = \sum_{r=1}^{n_x}\sum_{s=1}^{n_y} B_{r,s}(x,y)\,\mathbf{A}_{n1,r,s}, \quad \mathbf{A}_{n2}(x,y) = \sum_{r=1}^{n_x}\sum_{s=1}^{n_y} B_{r,s}(x,y)\,\mathbf{A}_{n2,r,s}.$$

Substituting Eq. (10) in the flutter equation (2), we obtain a nonlinear eigenvalue system of dimension $2\,m_n$ which depends explicitly on the parameters

$$\begin{bmatrix} \mathbf{0} & \mathbf{I} \\ -\mathbf{M}_{gn}^{*-1}(x,y)[\mathbf{K}_{gn}^{*}(x,y)+\mathbf{G}_n(p,x,y)] & -\mathbf{M}_{gn}^{*-1}(x,y)\mathbf{C}_{gn}^{*}(x,y) \end{bmatrix}\begin{Bmatrix} \tilde{\mathbf{q}}_n \\ p\tilde{\mathbf{q}}_n \end{Bmatrix} = p\begin{Bmatrix} \tilde{\mathbf{q}}_n \\ p\tilde{\mathbf{q}}_n \end{Bmatrix}, \tag{11}$$

with

$$\begin{aligned}
\mathbf{K}_{gn}^{*}(x,y) &= \mathbf{K}_{gn}(x,y) + \tfrac{1}{2}\rho_\infty V_\infty^2\,\mathbf{A}_{n0}(x,y),\\
\mathbf{C}_{gn}^{*}(x,y) &= \mathbf{C}_{gn}(x,y) + \tfrac{1}{2}\rho_\infty c\,V_\infty\,\mathbf{A}_{n1}(x,y),\\
\mathbf{M}_{gn}^{*}(x,y) &= \mathbf{M}_{gn}(x,y) + \tfrac{1}{2}\rho_\infty c^2\,\mathbf{A}_{n2}(x,y),\\
\mathbf{G}_n(p,x,y) &= \frac{1}{2}\rho_\infty V_\infty pc\sum_{r=1}^{n_x}\sum_{s=1}^{n_y} B_{r,s}(x,y)\mathbf{D}_{n,r,s}[(p\,c/V_\infty)\mathbf{I}-\mathbf{R}_{n,r,s}]^{-1}\mathbf{E}_{n,r,s}.
\end{aligned}$$

The nonlinear eigenvalue problem Eq. (11) is solved for any arbitrary computed point (x,y) and for various values of the fluid upstream infinite velocity V_∞ by using an iterative process based on the method of successive approximations for finding a fixed point of a function (Tran et al., 2003), providing the aeroelastic frequencies and dampings. The aeroelastic stability of the coupled system in the operating map can be studied, without having to perform any additional aerodynamic computations.

3.2. Multi-parameter minimum state modeling in time domain

To obtain the approximation in Eq. (8) of the matrix $\mathbf{A}_{n,r,s}(p)$, $n_{p,r,s}$ auxiliary state variables $\tilde{\mathbf{z}}_{n,r,s}$ have been defined for each couple $(r,s)\in\{1,\ldots,n_x\}\times\{1,\ldots,n_y\}$ by

$$\tilde{\mathbf{z}}_{n,r,s} = B_{r,s}(x,y)\,\frac{pc}{V_\infty}\left[\frac{pc}{V_\infty}\mathbf{I}-\mathbf{R}_{n,r,s}\right]^{-1}\mathbf{E}_{n,r,s}\tilde{\mathbf{q}}_n. \tag{12}$$

These auxiliary state variables in the frequency domain satisfy

$$p\tilde{\mathbf{z}}_{n,r,s} = (V_\infty/c)\mathbf{R}_{n,r,s}\tilde{\mathbf{z}}_{n,r,s} + pB_{r,s}(x,y)\mathbf{E}_{n,r,s}\tilde{\mathbf{q}}_n, \tag{13}$$

and they are solutions of a system of first-order differential equations in the time domain:

$$\dot{\mathbf{z}}_{n,r,s}(t) = (V_\infty/c)\mathbf{R}_{n,r,s}\mathbf{z}_{n,r,s}(t) + B_{r,s}(x,y)\mathbf{E}_{n,r,s}\dot{\mathbf{q}}_n(t). \tag{14}$$

The GAF are then written, respectively, in the frequency and time domains as

$$\tilde{\mathbf{F}}_{agn}(\mathbf{\Phi}_n, p, x, y)\tilde{\mathbf{q}}_n = -\frac{1}{2}\rho_\infty V_\infty^2 \left(\left[\mathbf{A}_{n0} + \frac{pc}{V_\infty}\mathbf{A}_{n1} + \frac{p^2c^2}{V_\infty^2}\mathbf{A}_{n2} \right] \tilde{\mathbf{q}}_n + \sum_{r=1}^{n_x}\sum_{s=1}^{n_y} \mathbf{D}_{n,r,s}\tilde{\mathbf{z}}_{n,r,s} \right), \tag{15}$$

$$\mathbf{f}_{agn}(\mathbf{\Phi}_n\mathbf{q}_n, \mathbf{\Phi}_n\dot{\mathbf{q}}_n, x, y) = -\frac{1}{2}\rho_\infty V_\infty^2 \left(\mathbf{A}_{n0}\mathbf{q}_n(t) + \frac{c}{V_\infty}\mathbf{A}_{n1}\dot{\mathbf{q}}_n(t) + \frac{c^2}{V_\infty^2}\mathbf{A}_{n2}\ddot{\mathbf{q}}_n(t) + \sum_{r=1}^{n_x}\sum_{s=1}^{n_y} \mathbf{D}_{n,r,s}\mathbf{z}_{n,r,s}(t) \right). \tag{16}$$

Substituting Eq. (16) in the reduced coupled system Eq. (1) and combining with Eq. (14), we obtain a linear system of second-order differential equations of dimension $m_n + n_p$ with $n_p = \sum_{r=1}^{n_x}\sum_{s=1}^{n_y} n_{p,r,s}$, which depends explicitly on the parameters x and y:

$$\begin{bmatrix} \mathbf{K}^*_{gn}(x,y) & \mathbf{D}'_n \\ \mathbf{0} & \mathbf{R}'_n \end{bmatrix} \begin{Bmatrix} \mathbf{q}_n \\ \mathbf{z}_n \end{Bmatrix} + \begin{bmatrix} \mathbf{C}^*_{gn}(x,y) & \mathbf{0} \\ \mathbf{E}'_n(x,y) & -\mathbf{I} \end{bmatrix} \begin{Bmatrix} \dot{\mathbf{q}}_n \\ \dot{\mathbf{z}}_n \end{Bmatrix} + \begin{bmatrix} \mathbf{M}^*_{gn}(x,y) & \mathbf{0} \\ \mathbf{0} & \mathbf{0} \end{bmatrix} \begin{Bmatrix} \ddot{\mathbf{q}}_n \\ \ddot{\mathbf{z}}_n \end{Bmatrix} = \begin{Bmatrix} \mathbf{f}_{gn} \\ \mathbf{0} \end{Bmatrix} \tag{17}$$

with $\mathbf{K}^*_{gn}(x,y)$, $\mathbf{C}^*_{gn}(x,y)$ and $\mathbf{M}^*_{gn}(x,y)$ defined as in Eq. (11), and

$$\mathbf{z}_n = {}^{\mathrm{t}}[{}^{\mathrm{t}}\mathbf{z}_{n,1,1}, \ldots, {}^{\mathrm{t}}\mathbf{z}_{n,1,n_y}, {}^{\mathrm{t}}\mathbf{z}_{n,2,1}, \ldots, {}^{\mathrm{t}}\mathbf{z}_{n,2,n_y}, \ldots, {}^{\mathrm{t}}\mathbf{z}_{n,n_x,1}, \ldots, {}^{\mathrm{t}}\mathbf{z}_{n,n_x,n_y}],$$
$$\mathbf{D}'_n = \tfrac{1}{2}\rho_\infty V_\infty^2[\mathbf{D}_{n,1,1}, \ldots, \mathbf{D}_{n,1,n_y}, \mathbf{D}_{n,2,1}, \ldots, \mathbf{D}_{n,2,n_y}, \ldots, \mathbf{D}_{n,n_x,1}, \ldots, \mathbf{D}_{n,n_x,n_y}],$$
$$\mathbf{R}'_n = (V_\infty/c)\,\mathrm{diag}(\mathbf{R}_{n,1,1}, \ldots, \mathbf{R}_{n,1,n_y}, \mathbf{R}_{n,2,1}, \ldots, \mathbf{R}_{n,2,n_y}, \ldots, \mathbf{R}_{n,n_x,1}, \ldots, \mathbf{R}_{n,n_x,n_y}),$$

$$\mathbf{E}'_n(x,y) = {}^{\mathrm{t}}[B_{1,1}(x,y)^{\mathrm{t}}\mathbf{E}_{n,1,1}, \ldots, B_{1,n_y}(x,y)^{\mathrm{t}}\mathbf{E}_{n,1,n_y}, B_{2,1}(x,y)^{\mathrm{t}}\mathbf{E}_{n,2,1},$$
$$\ldots, B_{2,n_y}(x,y)^{\mathrm{t}}\mathbf{E}_{n,2,n_y}, \ldots, B_{n_x,1}(x,y)^{\mathrm{t}}\mathbf{E}_{n[,n_x,1]}, \ldots, B_{n_x,n_y}(x,y)^{\mathrm{t}}\mathbf{E}_{n,n_x,n_y}].$$

This second-order system is solved using the Newmark numerical integration scheme for any arbitrary computed point (x, y).

Due to the nonlinear last term in Karpel's minimum state approximation, Eqs. (8) and (10), the multi-parameter modeling method is not equivalent to the mono-parameter method in which the rational approximation equation (6) is performed for each computed point.

4. Numerical application

The previously described multi-parameter modeling method using the spline approximation and the minimum state modeling have been applied to a numerical model of an aircraft engine compressor disk which is composed of 24 large-chord blades. The two parameters which are chosen to vary in the coupling calculations are the rotation speed Ω and the inter-blade phase angle σ_n, or equivalently, the phase number n. The initial values of these parameters are in $T_\Omega = \{70\,\mathrm{Nn}, 90\,\mathrm{Nn}\}$, Nn being a nominal rotation speed, and in $T_n = \{0, 1, 3, -1, -3\}$ for the phase number. A positive phase number corresponds to a forward wave traveling in the direction of the rotation (from suction side to pressure side), while a negative phase number corresponds to a backward wave traveling in the opposite direction.

4.1. Structural and aerodynamic computations

The structural finite element model of a reference sector with one blade has 154 332 degrees of freedom. The eigenfrequencies and modes in vacuum are computed by using the cyclic symmetry and by taking into account the geometrical stiffness matrix due to the centrifugal stress generated by the rotation. For the coupling calculations, the projection basis $\mathbf{\Phi}_n$ is composed of the first two bending modes (1F and 2F). The reduced eigenfrequencies of the two modes are shown in the Campbell diagrams in Fig. 1 for $n = 0, \ldots, 5$. The eigenfrequencies for the phase number n and $-n$ are the same, while the eigenmodes are complex conjugate.

In order to perform the unsteady aerodynamic computations to obtain the GAF, the structural eigenmodes are transferred to the fluid mesh at the blade profile. They are then normalized so that the maximum module of the complex displacements of the blade is equal to 1 mm. For nonzero phase numbers ($n \neq 0$), the complex modes are also

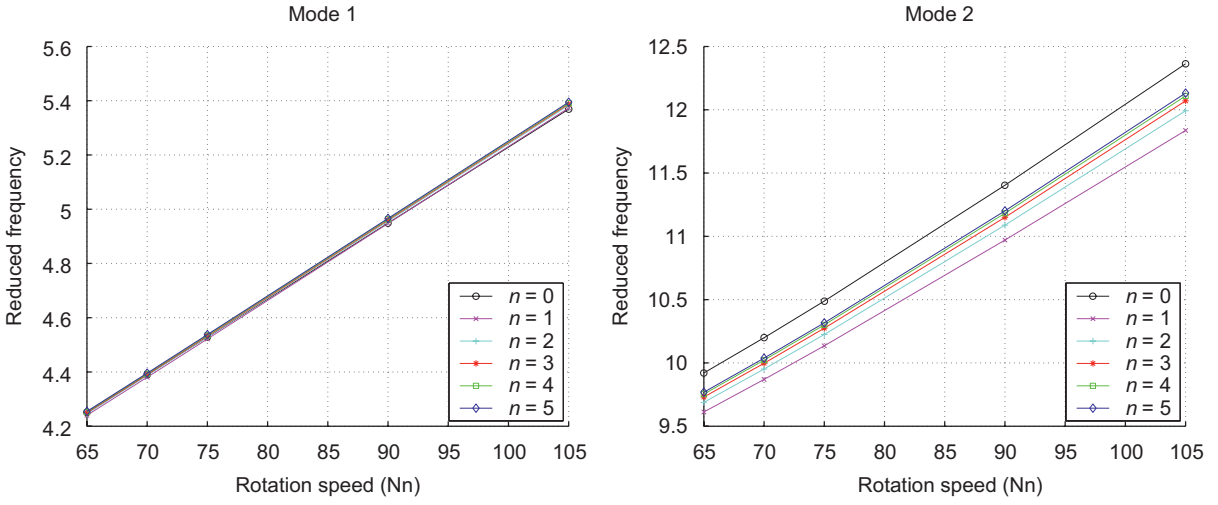

Fig. 1. Campbell diagrams.

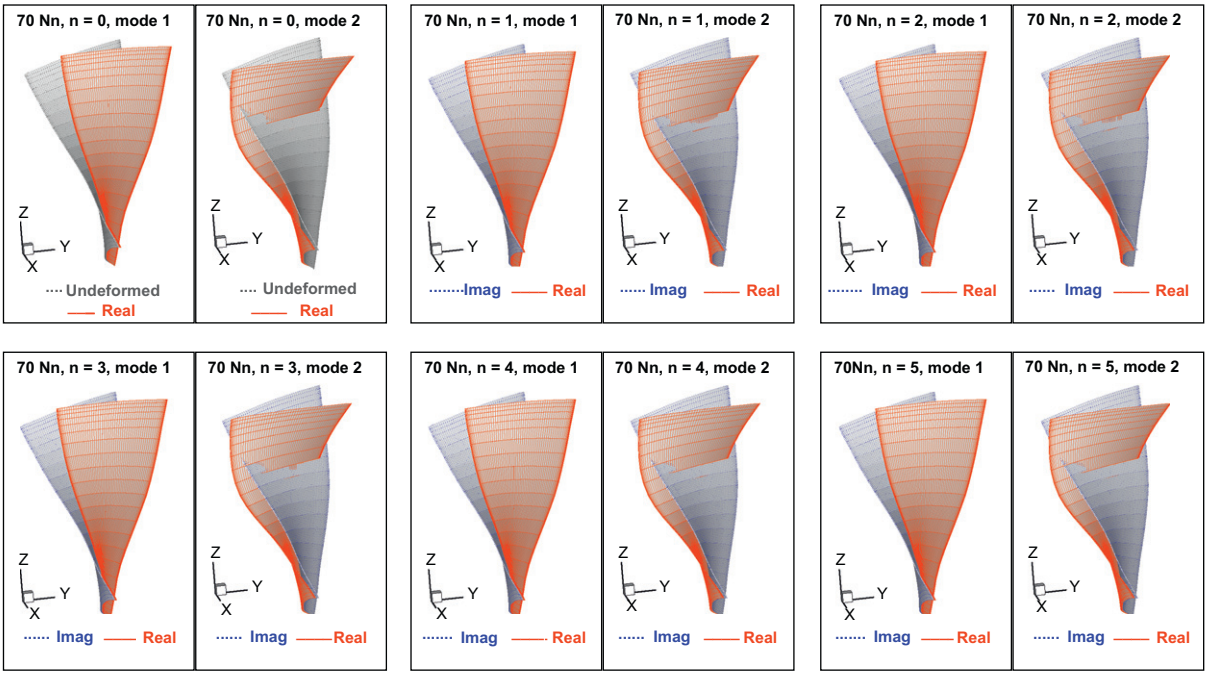

Fig. 2. Eigenmodes in vacuum for $\Omega = 70\,\mathrm{Nn}$.

normalized, by multiplying with a complex number with module equal to 1, i.e. by performing a rotation of the modes, so that the real part of the mode, which corresponds to the real, physical displacements of the reference sector, is similar the real mode obtained with $n = 0$. The first two bending modes on the fluid mesh at the blade profile are shown in Fig. 2 for $\Omega = 70\,\mathrm{Nn}$ and $n = 0, \ldots, 5$. We remark that the real parts of the modes are similar while the imaginary parts are very small compared to the real parts.

The Euler simulations are performed by using an aerodynamic code called CANARI and developed for years at ONERA (Dugeai et al., 2000). The mesh of one passage of the embedding fluid is a structured grid composed of six domains with 23 layers along the blade length, having in total 87 676 (3812×23) points, 1656 (72×23) of

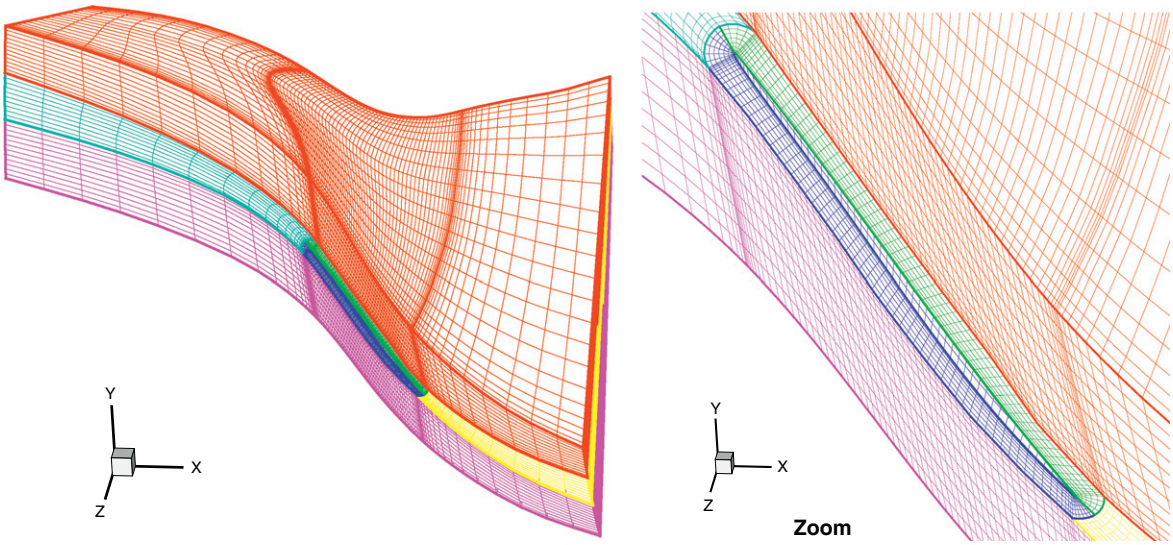

Fig. 3. Fluid mesh.

Table 1
Steady upstream infinite mass flow, velocity and absolute Mach number

Ω (Nn)	65	70	75	90	105
$MF_\infty/MF_{\infty\mathrm{ref}}$	0.838	0.922	1.000	1.215	1.279
$V_\infty/V_{\infty\mathrm{ref}}$	0.800	0.900	1.000	1.225	1.325
M_∞	0.32	0.36	0.41	0.50	0.55

which are on the pressure side and 1564 (68×23) on the suction side (Fig. 3). The following aerodynamic conditions are used:

Initial rotation speeds	Ω	$= 70$ and 90 Nn,
Upstream total temperature	T_{i1}	$= 293$ K,
Upstream total pressure	P_{i1}	$= 100\,630$ Pa,
Outlet/inlet pressure ratio	P_2/P_{i1}	$= 0.975$,
Flow axial direction		$= 0^\circ$,
Initial phase numbers	n	$= 0$, 1, 3, -1 and -3.

The steady aerodynamic computations are performed for the initial rotation speeds and also for the other computed rotation speeds $\Omega = 60$, 75 and 105 Nn. The upstream infinite fluid velocity V_∞ and mass flow MF_∞ obtained at $\Omega = 75$ Nn are chosen as the reference fluid velocity and mass flow, $V_{\infty\mathrm{ref}}$ and $MF_{\infty\mathrm{ref}}$, for adimensioning. The adimensioned steady upstream infinite mass flow, velocity and absolute Mach number are shown in Table 1.

With the steady flowfield previously computed and used as initial conditions, the unsteady aerodynamic simulations are performed at the 10 initial points $(\Omega, n) \in T_\Omega \times T_n$ by exciting the first two modes (1F and 2F) with a harmonic motion and the aerodynamic coefficient matrices are obtained by projecting the induced aerodynamic forces on these modes, using five reduced excitation frequencies $\kappa = 2\pi fc/V_{\infty\mathrm{ref}}$: 0.229, 4.349, 9.155, 14.65, 20.6. A blowing condition is used to simulate the blade motion.

The number of unsteady aerodynamic computations is 20 for $n = 0$ (2 rotation speeds $\times 2$ modes $\times 5$ frequencies) and 160 for $n \neq 0$ (2 rotation speeds $\times 4$ phase numbers $\times 4$ modes (real and imaginary parts) $\times 5$ frequencies). The number of oscillating periods, the number of time steps and the computation times on a HP-Itanium work station are shown in Table 2.

Table 2
Some statistics on the unsteady computations

Phase number	$n=0$				$n\neq0$			
Reduced frequency	0.229	4.349	9.155	14.65 and 20.6	0.229	4.349	9.155	14.65 and 20.6
Number of periods	4	10	40	40	20	20	40	40
Number of time steps per period	30 000	2040	1008	600	72[a]	72[a]	1008	600
Computation time (h)	11	2	3	2	13	4	4	3

[a]Dual time step.

The dual time step technique is used for the frequencies 0.229 and 4.349 in the case $n\neq0$. The time evolution of the aerodynamic coefficients is well stabilized at the end of the simulation.

For $n\neq0$, the aerodynamic coefficient matrices obtained by exciting and by projecting separately on the real and imaginary parts of the complex modes should be recomposed to obtain the matrices of GAF induced by the complex modes. The complex modes are normalized again, and the matrices of GAF are modified consequently by linearity, so that the generalized mass is equal to the identity matrix for all the cases. This is to insure the homogeneity of the reduced coupled system and the GAF, before performing the spline approximation and the solution of the coupled system. We notice that the GAF obtained by taking into account only the real parts of the modes are practically the same as those obtained previously by using both parts. This is explained by the fact that the imaginary parts of the modes are very small compared to the real parts. This also means that the unsteady aerodynamic computation costs can be divided by two in this case.

4.2. Coupling computations

The reduced coupled systems are solved for 45 computed points $(\Omega,n)\in\{65\,\text{Nn},\ 70\,\text{Nn},\ 75\,\text{Nn},\ 90\,\text{Nn},\ 105\,\text{Nn}\}\times\{-4,-3,-2,-1,0,1,2,3,4\}$ which include the 10 initial points (Fig. 4), by using Karpel's minimum state modeling method in both approaches: the multi-parameter method given in Eqs. (11) and (17) or the mono-parameter method which consists in performing Eq. (6) for each computed point. The spline approximations will be performed using spline functions of order 2 (linear approximation). The coupling computations are performed in both frequency and time domains for the following cases.

Case a: Initial points. The coupled system is solved only for the 10 initial points using the multi-parameter minimum state modeling method, with the 10 tabulated GAF matrices as input data. Since there is no extrapolation, the spline coefficient matrices are identical to the tabulated GAF matrices. This case is the same as the one where the mono-parameter minimum state modeling method is performed at each initial point, with the tabulated GAF matrices as input data.

Case b: Computed points, multi-parameter method. The coupled system is solved for the 45 computed points using the multi-parameter minimum state modeling method, with the 10 tabulated GAF matrices as input data. Due to the extrapolation, the spline coefficient matrices are no longer identical to the tabulated GAF matrices. The results are compared to the reference results of Case a for the initial points and of Case d for the verified points.

Case c: Computed points, mono-parameter method. The coupled system is solved for the 45 computed points using the mono-parameter minimum state modeling method, with the GAF matrices obtained at the computed points from the spline approximation as input data. Note that the spline approximation provides at the initial points the same GAF matrices as the tabulated ones, whatever the order of the spline functions and even in the case of extrapolation. The results at the initial points should be the same as the reference results of Case a.

Case d: Verified points. The results obtained in Cases b and c are compared to the reference results obtained at the verified points $(\Omega,n)\in\{(65\,\text{Nn},-2),\ (65\,\text{Nn},0),\ (70\,\text{Nn},4),\ (75\,\text{Nn},0),\ (75\,\text{Nn},2),\ (90\,\text{Nn},-4),\ (105\,\text{Nn},0),\ (105\,\text{Nn},4)\}$ (Fig. 4). At these points, the unsteady aerodynamic computations are performed to obtain the GAF matrices and the coupled system is then solved using the mono-parameter minimum state modeling method with these GAF matrices as input data. Note that the unsteady aerodynamic computations failed to converge at $\Omega=65\,\text{Nn}$ and by consequent the GAF matrices and the reference coupling results are not available for this rotation speed.

Depending on the coupling computation cases, Karpel's minimum state smoothing is performed either on the spline coefficient matrices or the GAF matrices, using six poles and with relative errors comprised between 0.4% and 2.9%.

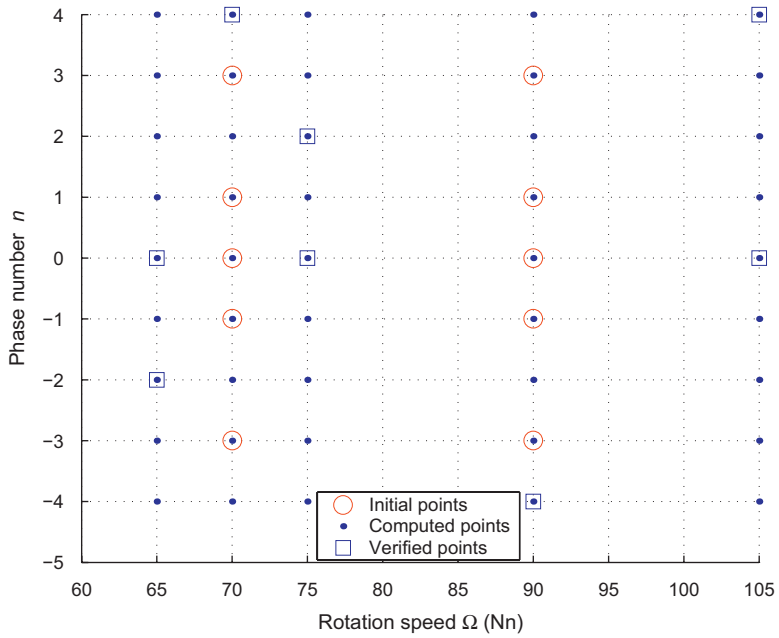

Fig. 4. Initial points, computed points and verified points.

At first, the coupled system is solved in the frequency domain. We obtain the flutter diagrams showing the variation of the aeroelastic frequencies and dampings in function of the upstream infinite fluid velocity and mass flow, around their "nominal" values obtained in the steady aerodynamic computations (Table 1). Fig. 5 shows the flutter diagrams at some initial points, and Fig. 6 at all the verified points. In all the figures, the aeroelastic dampings are scaled up so that their maximum values are equal to unity. The aeroelastic frequencies are the same for all the computation cases and they do not vary significantly with the upstream infinite fluid velocity. As for the aeroelastic dampings, Cases a and c give the same results at the initial points as expected. We also obtain a good accordance between Case b and Cases a and d. Some differences are observed on the dampings of the first mode at $\Omega = 70$ Nn, however, the dampings are very small at these points. At the verified points, the diagrams obtained in the three cases are very close or they have the same shape, except at the points (70 Nn, 4) and (75 Nn, 0). Here again, the dampings are very small at the last point. Moreover, Cases b and c give the same results for $\Omega = 105$ Nn. These flutter diagrams show that the aeroelastic system is stable around the nominal upstream infinite fluid velocity and mass flow, and that the first mode (1F) is more stable than the second mode (2F) in most of the cases.

Secondly, the coupled system is solved in the time domain at the nominal upstream infinite fluid velocity, and with the same GAF as in the frequency domain. The time step is obtained by dividing the period of the second mode by 60. The time responses of the generalized coordinates to an initial condition are shown in Fig. 7 for some initial and computed points. Here again the time responses obtained in the various cases are very close, and the system is stable in most of the cases, except at some isolated points such as (65 Nn, 1). The Fourier analysis of the signals is then performed to obtain the aeroelastic frequencies and dampings.

Both frequency and time domain methods and all the computation cases provide practically the same aeroelastic frequencies, the errors are in most of the cases less than 0.5%, with a maximum of 2%. For a given rotation speed, the aeroelastic frequencies vary very little with the phase number.

Fig. 8 shows the variation of the aeroelastic dampings obtained from both frequency and time domain methods, and scaled up with the same factor for both methods, in function of the phase number, for all the rotation speeds, as follows.

(i) For $\Omega = 65$ Nn, both Cases b and c and both frequency and time domain computations give very close results, except at $n = 3$ and 4 where the frequency domain method shows that the first mode is unstable. This is consistent with the fact that the unsteady aerodynamic computations failed to converge for this rotation speed. The time domain computations do not seem to predict any instability in Fig. 8, however, Fig. 7 shows that the time responses diverge at the point (65 Nn, 1), which means that the aeroelastic system is unstable at this point.

(ii) For $\Omega \neq 65$ Nn, the system is stable around the nominal upstream infinite velocity in all the cases. The damping of the first mode reaches a minimum at $n = 0$ and sometimes at $n = 1$. Here again, the results obtained at the computed

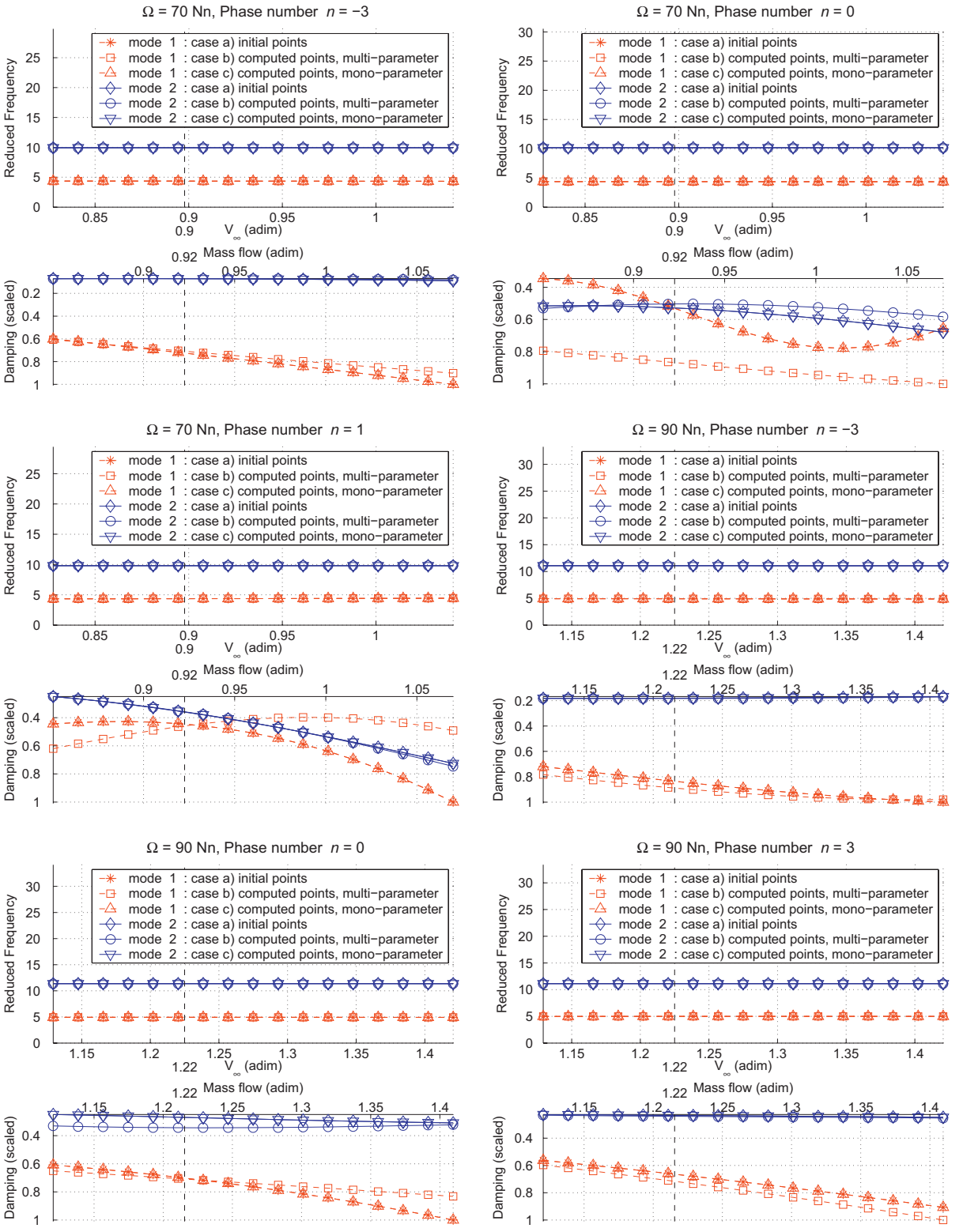

Fig. 5. Flutter diagrams at initial points.

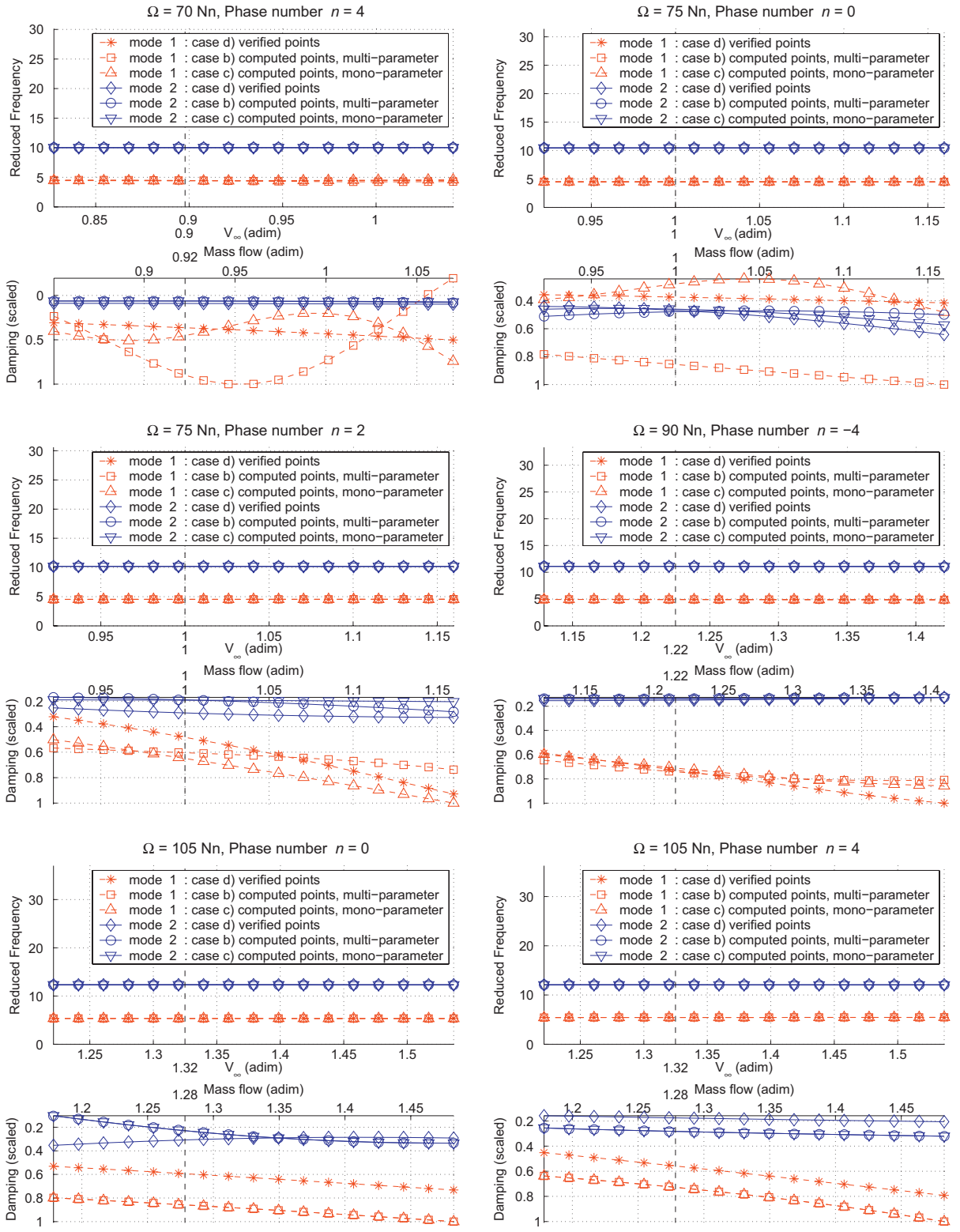

Fig. 6. Flutter diagrams at verified points.

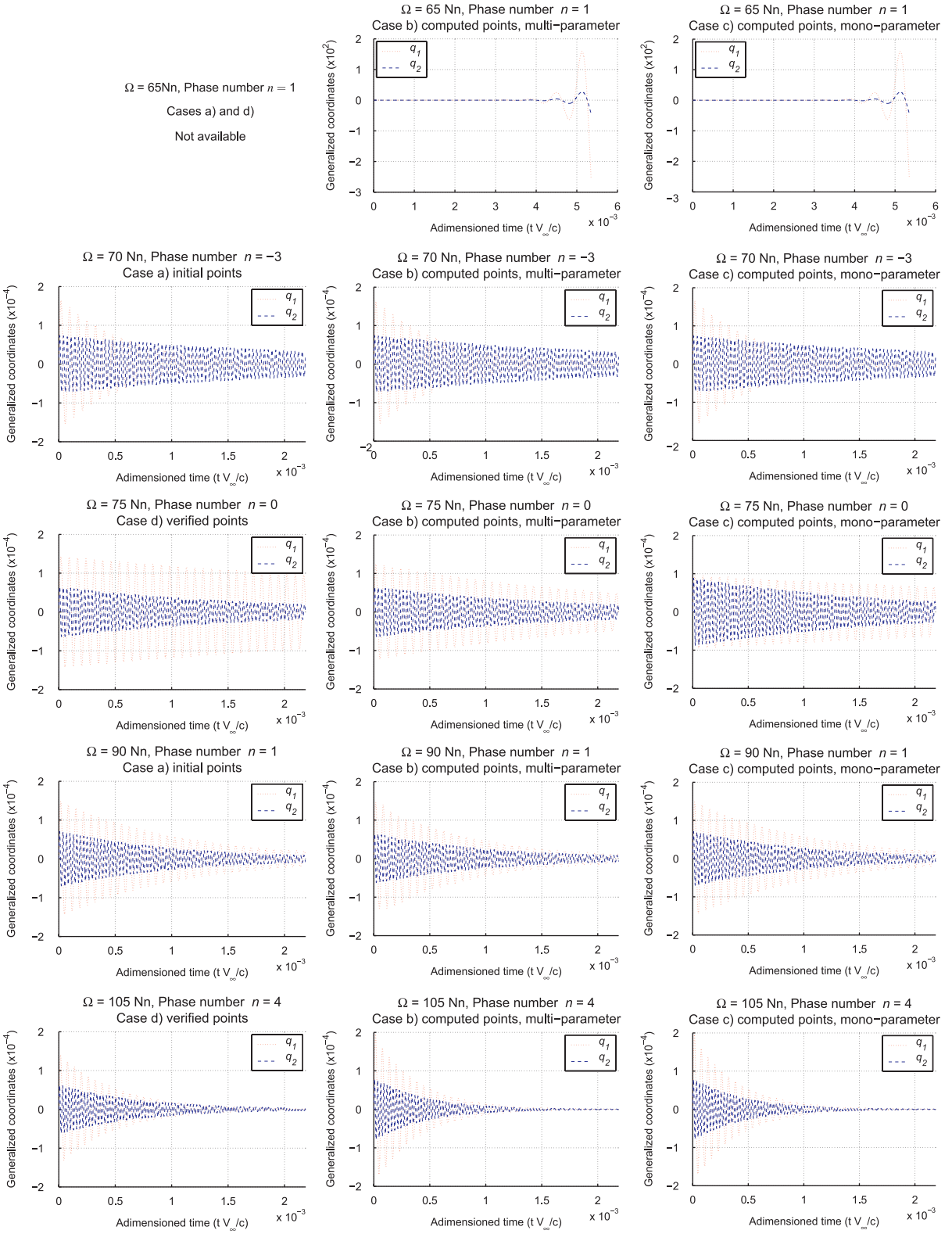

Fig. 7. Time responses of the generalized coordinates.

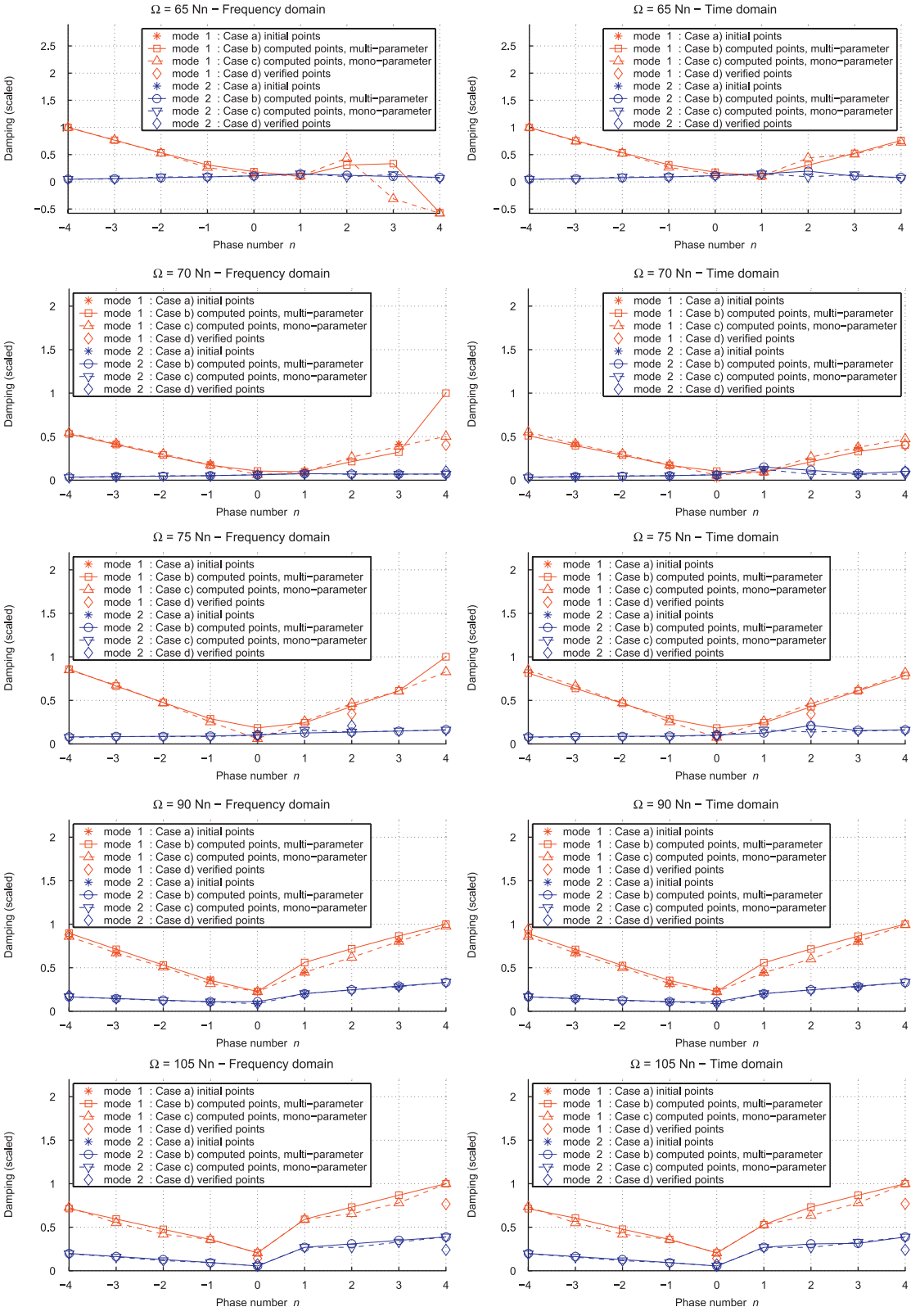

Fig. 8. Variation of the aeroelastic dampings in function of the phase number.

points in Cases b and c are in good accordance with the reference results at the initial and verified points in Cases a and d, except at some isolated points. At the point (70 Nn, 4) for example, the frequency domain computations do not give good results for Case d, but provide for Case c very good results which are close to the reference results of Case d. At the point (105 Nn, 4) on the other hand, both frequency and time domain methods give for Cases b and c the same results which differ to those of Case d. The mono-parameter method (Case c) is slightly better than the multi-parameter method (Case b) in this example. The results from the frequency and time domain methods are also in very good accordance, in particular both methods give the same positions of the less stable points with minimum dampings.

5. Conclusion

A multi-parameter minimum state modeling method is proposed to reduce the number and the cost of the aerodynamic computations in the solutions of the aeroelastic systems and it is applied to a compressor blade. The reduced coupled system is solved in both frequency and time domains at the computed points where aerodynamic computations are not performed. The results are in good accordance with the reference results at the initial and verified points where aerodynamic computations were performed to obtain the GAF. Another approach which consists in using the mono-parameter minimum state modeling method with the GAF obtained from the spline approximation also provides very good results. Using the extrapolation capability, both mono-parameter and multi-parameter minimum state modeling methods can predict unstable areas which are located outside the stable areas and where the aerodynamic computations cannot be achieved. Further works for reducing the aerodynamic computation cost will be the development of reduced order models of the fluid domain.

Acknowledgments

The author thanks the "Direction des Programmes Aéronautiques et de la Coopération (DGAC/DPAC)" and the "Services de Programmes Aéronautiques (SPAé)" for their financial support, and "SNECMA, Groupe SAFRAN" (Villaroche, France) for providing the test-case data.

References

Attar, P.J., Dowell, E.H., 2005. A reduced order system ID approach to the modelling of nonlinear structural behavior in aeroelasticity. Journal of Fluids and Structures 21 (5–7), 532–542.

Carstens, V., Kemme, R., Schmitt, S., 2003. Coupled simulation of flow–structure interaction in turbomachinery. Aerospace Science and Technology 7, 298–306.

Craig Jr., R.R., Bampton, M.C.C., 1968. Coupling of substructures for dynamic analysis. AIAA Journal 6 (7), 1313–1319.

Crawley, E.F., 1988. Aeroelastic formulation for tuned and mistuned rotors. AGARD-AG-298, vol. 2, pp. 19.1–19.24.

Dat, R., Meurzec, J.-L., 1969. Sur les calculs de flottement par la méthode dite du "balayage en fréquence réduite". La Recherche Aérospatiale, No. 133, pp. 41–43.

de Boor, C., 1992. Spline Toolbox for Use with Matlab, User's Guide. The Math Works Inc.

de Boor, C., 2001. A Practical Guide to Spline, revised ed. Applied Mathematical Sciences, vol. 27, Springer, Berlin.

Dugeai, A., 2005. Aeroelastic developments in the elsA code and unsteady RANS applications. In: Proceedings of the International Forum on Aeroelasticity and Structural Dynamics, Munich, Germany.

Dugeai, A., 2008. Nonlinear numerical aeroelasticity with the ONERA elsA solver. In: NATO Specialists Meeting RTO-AVT-154 Advanced Methods in Aeroelasticity, Loen, Norway, pp. 12.1–12.17.

Dugeai, A., Madec, A., Sens, A.S., 2000. Numerical unsteady aerodynamics for turbomachinery aeroelasticity. In: Ferrand, P., Aubert, S. (Eds.), Proceedings of the Ninth International Symposium on Unsteady Aerodynamics, Aeroacoustics and Aeroelasticity of Turbomachines, Lyon, France, PUG, pp. 830–840.

Epureanu, B.I., 2003. A parametric analysis of reduced order models of viscous flows in turbomachinery. Journal of Fluids and Structures 17 (7), 971–982.

Epureanu, B.I., Dowell, E.H., Hall, K.C., 2000. Reduced-order models of unsteady transonic viscous flows in turbomachinery. Journal of Fluids and Structures 14 (8), 1215–1234.

Epureanu, B.I., Hall, K.C., Dowell, E.H., 2001. Reduced-order models of unsteady viscous flows in turbomachinery using viscous–inviscid coupling. Journal of Fluids and Structures 15 (2), 255–273.

Gnesin, V.I., Kolodyazhnaya, L.V., Rzadkowski, R., 2004. A numerical modelling of stator–rotor interaction in a turbine stage with oscillating blades. Journal of Fluids and Structures 19 (2), 1141–1153.

Grisval, J.-P., Liauzun, C., 1999. Application of the finite element method to aeroelasticity. Revue Européenne des Éléments Finis 8 (5–6), 553–579.

Grisval, J.P., Liauzun, C., 2000. Unsteady viscous flow in turbomachinery cascade: a finite element approach. In: Proceedings of the Eighth International Symposium on Transport Phenomena and Dynamics of Rotating Machinery, vol. 1, ISROMAC-8, Hawaii, pp. 407–412.

He, Z., Epureanu, B.I., Pierre, C., 2007. Parametric study of the aeroelastic response of mistuned bladed disks. Computers and Structures 85, 852–865.

He, Z., Epureanu, B.I., Pierre, C., 2008. Convergence predictions for aeroelastic calculations of tuned and mistuned bladed disks. Journal of Fluids and Structures 24 (5), 732–749.

Jacquet-Richardet, G., Rieutord, P., 1998. A three-dimensional fluid–structure coupled analysis of rotating flexible assemblies of turbomachines. Journal of Sound and Vibration 209 (1), 61–76.

Karpel, M., 1982. Design for active flutter suppression and gust alleviation using state-space aeroelastic modeling. AIAA Journal of Aircraft 19, 221–227.

Liauzun, C., Tran, D.-M., 2002. Method of fluid structure coupling in time domain using linearized aerodynamics for turbomachineries. In: Proceedings of the 2002 ASME International Engineering Congress and Exposition, vol. 3, New Orleans, LA, USA.

Marshall, J.G., Imregun, M., 1996. Review of aeroelasticity methods with emphasis on turbomachinery applications. Journal of Fluids and Structures 10 (3), 237–267.

Moffatt, S., He, L., 2005. On decoupled and fully-coupled methods for blade forced response prediction. Journal of Fluids and Structures 20 (2), 217–234.

Poirion, F., 1995. Modélisation temporelle des systèmes aéroservoélastiques. Application à l'étude des effets des retards. La Recherche Aérospatiale, No. 2, pp. 103–114.

Poirion, F., 1996. Multi-mach rational approximation to generalized aerodynamic forces. AIAA Journal of Aircraft 33, 1199–1201.

Roberts, R.P., 1991. The application of the minimum state method for approximating unsteady aerodynamics to an aircraft model. In: Proceedings of the European Forum on Aeroelasticity and Structural Dynamics, Aachen, Germany.

Rzadkowski, R., Gnesin, V., 2007. 3-D inviscid self-excited vibrations of a blade row in the last stage turbine. Journal of Fluids and Structures 23 (6), 858–873.

Sarkar, S., Venkatraman, K., 2004. Model order reduction of unsteady flow past oscillating airfoil cascades. Journal of Fluids and Structures 19 (2), 239–247.

Sayma, A.I., Vahdati, M., Imregun, M., 2000. An integrated nonlinear approach for turbomachinery forced response prediction. Part I: formulation. Journal of Fluids and Structures 14 (1), 87–101.

Thomas, D.L., 1979. Dynamics of rotationally periodic structures. International Journal for Numerical Methods in Engineering 14, 81–102.

Tran, D.-M., 2001. Component mode synthesis methods using interface modes. Application to structures with cyclic symmetry. Computers and Structures 79 (1), 209–222.

Tran, D.-M., Liauzun, C., 2003. Frequency and time domain fluid–structure coupling methods for turbomachineries. In: Proceedings of the 10th International Symposium on Unsteady Aerodynamics, Aeroacoustics and Aeroelasticity of Turbomachines ISUAAAT. Duke University, Durham, NC, USA.

Tran, D.-M., Liauzun, C., Labaste, C., 2003. Methods of fluid–structure coupling in frequency and time domains using linearized aerodynamics for turbomachinery. Journal of Fluids and Structures 17 (8), 1161–1180.

Tran, D.-M., Poirion, F., Liauzun, C., 2004. Method of fluid–structure coupling for turbomachinery with multi-parameter modeling of generalized aerodynamic forces. In: Proceedings of the Sixth World Congress on Computational Mechanics WCCM VI and APCOM'04, Beijing, China.

Tran, D.-M., Poirion, F., Liauzun, C., 2005. Multi-parameter aerodynamic modeling for fluid–structure coupling in turbomachinery. In: Proceedings of the Seventh International Symposium on Experimental and Computational Aerothermodynamics for Internal Flows ISAIF7, Tokyo, Japan.

Valid, R., Ohayon, R., 1985. Théorie et calcul statique et dynamique des structures à symétries cycliques. La Recherche Aérospatiale, No. 4, pp. 251–263.

Willcox, K., 2000. Reduced-order aerodynamic models for aeroelastic control of turbomachines. Ph.D. Thesis, Department of Aeronautics and Astronautics, Massachusetts Institute of Technology, Cambridge, MA, USA.